The Meteoritical Society

Meteoritics & Planetary Science 44, Nr 12, 1877–1887 (2009)
Abstract available online at http://meteoritics.org

The formation of the Baptistina family by catastrophic disruption: Porous versus non-porous parent body

Martin JUTZI[1, 2], Patrick MICHEL[2*], Willy BENZ[1], and Derek C. RICHARDSON[3]

[1]Physikalisches Institut, University of Bern, Sidlerstrasse 5, 3012 Bern, Switzerland
[2]University of Nice-Sophia Antipolis, CNRS/UMR 6202 Cassiopée, Côte d'Azur Observatory, BP 4229, 06304 Nice Cedex 4, France
[3]Department of Astronomy, University of Maryland, College Park, Maryland 20742, USA
*Corresponding author. E-mail: michel@oca.eu

(Received 27 November 2008; revision accepted 30 August 2009)

Abstract–In this paper, we present numerical simulations aimed at reproducing the Baptistina family based on its properties estimated by observations. A previous study by Bottke et al. (2007) indicated that this family is probably at the origin of the K/T impactor, is linked to the CM meteorites and was produced by the disruption of a parent body 170 km in size due to the head-on impact of a projectile 60 km in size at 3 km s^{-1}. This estimate was based on simulations of fragmentation of non-porous materials, while the family was assumed to be of C taxonomic type, which is generally interpreted as being formed from a porous body. Using both a model of fragmentation of non-porous materials, and a model that we developed recently for porous ones, we performed numerical simulations of disruptions aimed at reproducing this family and at analyzing the differences in the outcome between those two models.

Our results show that a reasonable match to the estimated size distribution of the real family is produced from the disruption of a porous parent body by the head-on impact of a projectile 54 km in size at 3 km s^{-1}. Thus, our simulations with a model consistent with the assumed dark type of the family requires a smaller projectile than previously estimated, but the difference remains small enough to not affect the proposed scenario of this family history.

We then find that the break-up of a porous body leads to different outcomes than the disruption of a non-porous one. The real properties of the Baptistina family still contain large uncertainties, and it remains possible that its formation did not involve the proposed impact conditions. However, the simulations presented here already show some range of outcomes and once the real properties are better constrained, it will be easy to check whether one of them provides a good match.

INTRODUCTION

Asteroids in the main belt are subjected to collisions that sometimes lead to the formation of an asteroid family, identified as a group of small bodies that share the same spectral and orbital properties. More than 20 asteroid families have now been discovered, and each is believed to be the outcome of the catastrophic breakup of a large parent body as a result of a collision with a smaller projectile. The collisional process is still poorly understood and while impact experiments in laboratories can allow us to improve our understanding at small scales, asteroid families are the best tool that Nature offers us to study it at large scales. In recent years, we have been able to reproduce successfully by numerical simulations of the large-scale collisional process some of the main asteroid families belonging to the S taxonomic type (Michel et al. 2001, 2002, 2003, 2004a, 2004b). Using a 3D SPH hydrocode that includes a model of fragmentation of brittle non-porous material (Benz and Asphaug 1994) and a gravitational *N*-body code to compute the gravitational interaction of the generated fragments, we found that most of the family members are the product of the gravitational reaccumulation of smaller fragments resulting from the target disruption. Thus, these simulations suggest that large family members should not be monolithic but rather consist of gravitational aggregates or so-called rubble piles. Simulations using the same method were then performed by Durda et al. (2004) who investigated the efficiency of satellite formation during catastrophic disruptions, and then later (Durda et al. 2007) characterized the size frequency distributions of fragments over a wide range of impact conditions. Nesvorný et al. (2006) applied also the same method to revisit the formation of the Karin family on the basis of an updated identification of the real members. Finally Leinhardt and Stewart (2009) developed another hybrid method (using the hydrocode called CTH instead of a 3D SPH one) to study other collisional phenomena such as the collision outcomes of primordial outer Solar System bodies.

However, so far, models of fragmentation did not include microporosity effects and therefore were adapted to non-porous brittle material. Consequently, they were only adapted to the study of the formation of families of bright taxonomic type (e.g., S-type), which are believed to be formed by the disruption of a non-porous parent body (a definition of porous versus non-porous will be given later). The low bulk densities measured for dark-type (e.g., C) asteroids, typically about 1.3 g/cm^3 (e.g., the asteroid Mathilde whose density was estimated by the NEAR mission; Yeomans et al. 1997) suggest that bodies of these types contain a large fraction of porosity (see also Britt and Consolmagno 2000). To investigate the formation of a dark-type (e.g. C, D) asteroid family, which involves the disruption of a porous parent body, it is necessary to account for the crushing of pores in the fragmentation phase and therefore another model, adapted to porous materials, is required to simulate this process.

While porosity at large scales can be modeled explicitly by introducing macroscopic voids, porosity on a scale much smaller than the numerical resolution has to be modeled through a different approach. The P-alpha model originally proposed by Herrmann (1969) and later modified by Carroll and Holt (1972) has been developed to provide a description of microscopic porosity with pore sizes beneath the spatial resolution of the numerical scheme (sub-resolution porosity) and smaller than the thickness of the shock front. Other models have also been developed, such as the one proposed by Sirono (2004) who studied low-velocity collisions between porous aggregates and Wünneman et al. (2006) who studied crater formation. We have recently developed a model for porous material based on the P-alpha one (Jutzi et al. 2008). For a greater reliability, we performed a validation at laboratory scale by comparison to impact experiments on porous pumice (Jutzi et al. 2009). Thus, we are now ready to apply our method at large scales.

A validation of our model for porous bodies at asteroid scale should consist of reproducing a well-identified dark-type family, as we did for S-type ones (e.g., Michel et al. 2001). However, before doing so in future work, we concentrate on a family whose identification and spectral type may still be subjected to revision, and which may be at the origin of the K/T impactor (Bottke et al. 2007) and CM meteorites. The fact that the taxomic type of this family, called Baptistina, is not yet firmly established, despite the assumption by Bottke et al. (2007) that it is a C-type one, makes it also interesting because our numerical simulations of disruption using different internal models of the parent body can provide some constraints. Indeed, we can consider different possibilities to model the parent body of this family, in particular a porous and a non-porous one, and test the sensitivity of the outcome on these models. Ideally, we can also determine which model best matches the observational estimate of the family properties. Ideally, we should use a wide range of possible internal structures of the parent body (i.e., monolithic, rubble pile, more or less porous) to perform the simulations, but for a a first application of our model of fragmentation of porous material at asteroid scales, we choose to put more effort on the use of this model in this paper, given also the large CPU time required to perform simulations.

In the following, we first summarize the properties currently estimated for the real Baptistina family. Then, we describe our method and simulations of the formation of this family starting from either a non-porous or a porous parent body. A discussion based on these results is then presented, followed by conclusions and perspectives.

THE BAPTISTINA FAMILY: ESTIMATED PROPERTIES FROM OBSERVATIONS

The Baptistina family is of particular interest as it was found by Bottke et al. (2007) to be a likely origin of the impactor that produced the Cretaceous/Tertiary (K/T) mass extinction event 65 Myr ago. The authors estimated that the formation of the family occurred 160 Myr ago and involved a parent body of 170 km in diameter. They also characterized this family as a C-type one, suggesting that the parent body was probably porous (see the Numerical Simulations of the Baptistina Family Formation section for a definition of porosity) and that the family is connected to the CM meteorites.

To characterize the size distribution of the real family members, Bottke et al. (2007) converted their absolute magnitude to diameter by assuming an albedo of 0.04, and then considered only objects with semi-major axis greater than 2.2638 AU. Then, they doubled this population, except the largest member (298) Baptistina (see Bottke et al. (2007) for more detailed explanations and justifications). In the following, for comparison, their estimated size distribution will be represented on each plot showing the outcome of our simulations. Note that the authors provided a best fit of this size distribution from a suite of simulations of disruptions of 100 km size non-porous (basalt) asteroids. The result of each simulation was scaled and compared to the family size distribution to estimate the true size of the parent body. Then, their best-fit run indicated that the Baptistina family was created by the head-on impact of a 60 km projectile at 3 km s^{-1}. The authors noted that there is a mismatch between the largest remnant of the best-fit size distribution and the family one, as they differ in diameter by a factor 1.6, but they decided that this was not an issue as these objects comprise less than 1% of the parent body's total mass. Therefore, in the following, we will consider satisfying the results of our simulations which also produce a largest remnant whose diameter differ from the estimated real one by a same factor.

There are still some uncertainties in the identification and spectra of the Baptistina family, despite the investigations by Bottke et al. (2007). Indeed, it was first found (Mothé-Diniz et al. 2005) that a few members of the family had a bright taxonomic type (e.g., S, V, A), but Bottke et al. (2007) claimed that these objects are interlopers that do not actually belong to the family. Other asteroids, i.e., (298) Baptistina and (2093) Genichesk, do belong to the family and their spectral types were characterized as Xc and C, respectively. Then, discussing the biases of the different surveys, e.g. SMASSII (Bus et al. 2002) and SDSS (Ivezic et al. 2001), which affect the discovery efficiency of different taxonomic types, Bottke et al. (2007) concluded that the Baptistina family should be considered as a C-complex family. The reason why the spectral properties of family members appear to range from C-types to Xc-types remains unclear, and the authors suggested that it could be due to the original location of the fragments in the interior of the parent body, which is likely to have experienced degrees of heating and aqueous alteration at depth. Despite this range of types, according to this study and for our purpose, this family should be considered as a dark type one, justifying the choice of a porous parent body to start with. Note however that Bottke et al. (2007) used the outcomes of simulations of a non-porous parent body breakup to compare with the real family, as no model of fragmentation of porous material was included in their numerical code of fragmentation. As we will see, the conclusions of their work may not suffer much from this inconsistency.

However, this is not the end of the story. The albedo of the largest member of the family, the asteroid Baptistina itself, is not known yet and thus both its size and spectral type may be revised in the future. Since the assumed albedo used to estimate the current size of the asteroid was in the low range (to be consistent with a dark classification), if the real albedo value is higher, then this asteroid would actually be smaller than currently estimated, and this would have interesting consequences for some results of our investigations, as we will see later. Moreover, Reddy et al. (2008) found that the asteroid Baptistina may actually be of S-type, instead of C-type, based on its visible spectrum, which shows a hint of a weak 0.9 μm feature, indicative of a S-type classification. They then provided an estimate of the albedo, about 0.14, which is much higher than the one associated to C-types, but they also recognized that it might not be reliable as there was some scatter in the data because of poor weather conditions. Nevertheless, these recent observations re-open the debate about the homogeneity of this family and its characterization as a C-type one. As for the possibility that there is a mixture of types in the family members, we will use the argument by Bottke et al. (2007) that it may be due to the location of the fragments within the parent body, and will consider it as a second-order effect with respect to the global property of the family (dark versus bright type). Then, in the next section, to account for the uncertainty in the classification of the family as a bright or dark type, we will consider two different kinds of parent bodies, a non-porous one to represent a bright type object, and a porous one to represent a dark type one. Being interested in determining the difference in the outcome from two well-defined models implying two different fragmentation processes, we do not consider in this paper the possibility that the parent body was a mixture of the two, which would add complexity and free parameters.

NUMERICAL SIMULATIONS OF THE BAPTISTINA FAMILY FORMATION

In order to perform simulations of the Baptistina family formation, we use a method and numerical codes based on the ones that have already allowed us to simulate successfully the formation of major bright-type asteroid families in different impact energy regimes (Michel et al. 2001, 2002, 2003, 2004a, 2004b). More precisely, our method consists of dividing the process in two phases: a fragmentation phase computed by a 3D SPH hydrocode (Benz and Asphaug 1994; Jutzi et al. 2008), and a gravitational phase computed by the gravitational *N*-body code *pkdgrav* (Richardson et al. 2000) during which fragments can interact with each other due to their mutual gravity and collisions. Our hydrocode was originally limited to addressing the fragmentation of brittle non-porous materials. While this is appropriate for modeling the formation of asteroid families of S taxonomic type, which are believed to result from the disruption of a non-porous parent body, this model is not adapted for addressing the formation of asteroid families produced by porous parent bodies, such as those of dark taxonomic type (e.g., C, D). For this, a model of fragmentation of porous bodies (which accounts for the crushing of pores in addition to the damage caused by the activation of cracks) is required and such a model has been developed and tested recently at laboratory scale (Jutzi et al. 2008, 2009). In the following we give a short overview of our method and codes, and then present our simulations.

Numerical Models of Fragmentation

Classical Model of Brittle Failure

To compute the fragmentation phase of the collision, we use a smoothed particle hydrodynamics (SPH) code. The standard gas dynamics SPH approach was extended by Benz and Asphaug (1994, 1995) to include an elastic-perfectly plastic material description (see e.g., Libersky and Petschek 1991) and a model of brittle failure based on the one of Grady and Kipp (1980). The so-called Tillotson equation of state for basalt (Tillotson 1962) is used to relate the pressure to density and internal energy. Material properties are also considered to be those of basalt, as they permit validation of the numerical model at laboratory scale (Benz and Asphaugh 1994) by comparison with impact experiments on basalt targets by Nakamura and Fujiwara (1991). We refer the reader to the paper by Benz and Asphaug (1994) for a detailed description of this code.

Model Including Porosity

Recently, our SPH impact code has been extended to include a model adapted for porous materials (Jutzi et al. 2008, 2009). Before presenting its main principles, we first define what is meant here by porosity. The scale of porosity must be defined in comparison with the other relevant dimensions involved in the problem, such as the size of the projectile and/or crater, etc. In particular, we define microscopic porosity as a type of porosity characterized by pores sufficiently small that their distribution can be assumed uniform and isotropic over these relevant scales. In particular, the sizes of the pores are in this case smaller than the thickness of the shock front. In this paper, a porous parent body is considered to contain such microporosity. Macroscopic porosity on the other hand is characterized by pores with sizes such that the medium can no longer be assumed to have homogeneous and isotropic characteristics over the scales of interest. In this case, pores have to be modeled explicitly and the hydrocode as described previously, which includes a model of non-porous brittle solids, can still be used. The presence of these large macroscopic voids will only affect the transfer efficiency and the geometry of the shock wave resulting from the impact, which can be computed using the existing code. This was done by Michel et al. (2003, 2004) to model the disruption of pre-shattered parent bodies of S-type families. We will not consider this kind of model in this paper. On the other hand, a body containing microporosity may be crushable: cratering on a microporous asteroid might be an event involving compaction rather than ejection (Housen et al. 1999). Thus, in an impact into a microporous material, a part of the kinetic energy is dissipated by compaction, which can lead to less ejection and lower speeds of the ejected material. These effects cannot be reproduced if hydrocodes developed for the modeling of non-porous solids are used, even using the same bulk density for the object. Therefore, a model is needed that takes pore compaction into account.

Our model is based on the so-called P-alpha model initially proposed by Herrmann (1969) and later modified by Carroll and Holt (1972). A detailed description of the model and its implementation in our SPH hydrocode can be found in Jutzi et al. (2008).

The original idea at the origin of the P-alpha model is based on the separation of the volume change in a porous material into two parts: the pore collapse on one hand and the compression of the material composing the matrix on the other hand. This separation can be achieved by introducing the so-called distention parameter a defined as $\alpha = \rho_s/\rho$, where ρ is the density of the porous material and ρ_s is the density of the corresponding solid (matrix) material. Distention can be converted to porosity using the relation $(1–1/\alpha)$.

The distention parameter α is then used in the computation of the pressure and the deviatoric stress tensor. Damage then increases as a result of both crack activation and change in the distension. As material parameters, we use the ones involved in our successful validation of the model by comparison with laboratory impact experiments on porous pumice (Jutzi et al. 2009).

Numerical Model of the Gravitational Phase

Once the collision is over and fracture ceases, the hydrodynamical simulations are stopped and intact fragments (if any) are identified. These fragments as well as single particles and their corresponding velocity distribution are fed into an *N*-body code that computes the dynamical part of the evolution of the system to late time. Note that since the total mass is fixed, the extent of the reaccumulation is entirely determined by the velocity field imposed by the collisional physics upon the individual fragments.

Since we are dealing with a fairly large number of bodies (typically a few hundreds of thousands) that we want to follow over long periods of time, we use a parallel *N*-body hierarchical tree code (e.g., Richardson et al. 2000) to compute the dynamics. The tree component of the code provides a convenient means of consolidating forces exerted by distant particles, reducing the computational cost. The parallel component divides the work evenly among available processors, adjusting the load each timestep according to the amount of work done in the previous force calculation. The code uses a straightforward second-order leapfrog scheme for the integration and computes gravity moments from tree cells to hexadecapole order. Particles are considered to be finite-sized hard spheres and collisions are identified each step using a fast neighbor-search algorithm. The code then detects and treats collisions and mergers between particles on the basis of different options that were investigated by Michel et al. (2002) for monolithic parent bodies. Here we use a treatment in which a criterion based on relative speed and angular momentum is applied: fragments are allowed to merge only if their relative speed is smaller than their mutual escape speed and the resulting spin of the merged fragment is smaller than the threshold value for rotational fission. When two particles merge, they are replaced by a single spherical particle with the same momentum. Non-merging collisions are modeled as bounces between hard spheres whose post-collision velocities are determined by the amount of dissipation occurring during the collisions. The latter is determined in our simulations by the coefficients of restitution in the tangential and normal directions of the velocity vectors relative to the point of contact (see Richardson 1994 for details). The values of these coefficients

Table 1. Impact conditions and largest remnant mass for all the simulations presented in this paper. The bulk density of both the projectile and targets $\rho_{t,p}$ (set equal in all cases), the projectile's radius R_p, the impact angle θ, the specific impact energy Q and the mass ratio of the largest remnant to the parent body M_{lr}/M_{pb} obtained by our simulations are indicated. The different label numbers of the models of parent bodies discriminate between the different impact conditions (projectile's size and impact angle).

Model	$\rho_{t,p}$ (g/cm^3)	R_p (km)	θ (°)	Q (erg/g)	M_{lr}/M_{pb}
Non-porous 1	2.7	30	0	1.98×10^9	6.5×10^{-3}
Non-porous 2	2.7	44	45	6.24×10^9	6.7×10^{-3}
Porous 1	1.3	22.5	0	8.35×10^8	4.7×10^{-2}
Porous 2	1.3	23.5	0	9.50×10^8	1.3×10^{-2}
Porous 3	1.3	25	0	1.15×10^9	5.7×10^{-3}
Porous 4	1.3	27	0	1.44×10^9	5.1×10^{-3}
Porous 5	1.3	30	0	1.98×10^9	3.2×10^{-3}
Porous Ob	1.3	35	45	3.20×10^9	2.2×10^{-2}

are poorly constrained. In the following, we choose to set the normal coefficient of restitution to 0.3 in the porous case, and to 0.5 in the non-porous one, and the tangential one to 1, meaning there is no surface friction (see also Michel et al. 2002). Note that we made a simulation using the value of 0.5 for the normal coefficient of restitution in the porous case, and found similar results as with the lower value. Michel et al. (2002) made simulations using a non-porous parent body and noted also that the outcomes were not sensitive to the adopted value of the normal coefficient set between 0.5 and 0.8.

Richardson et al. (2009) have recently improved the *N*-body code by adding a model for rigid aggregates, which allows particles to stick (or bounce) at contact and thus grow aggregates of different shapes. Although this improvement allows a determination of shape and spins of family fragments, it involves a great number of parameters and heavy computations, and several tests are still necessary. Hence, we do not use it here but leave its application for future work.

All the *N*-body simulations presented in this paper were performed using a conservative integration stepsize of 5 seconds and were run to late times from a few days to a few tens of days as indicated on the following plots, and at least until there was no change anymore in the outcome.

Material Parameters and Initial Conditions

We performed the simulations of the Baptistina family formation starting from a parent body with a diameter of D = 170 km, following the estimate made by Bottke et al. (2007). We then considered two kinds of material composing the parent body:

- Solid material (basalt), initial density: ρ = 2.7 g/cm^3 (labeled Non-porous)
- Porous material (pumice), initial density ρ = 1.3 g/cm^3 (labeled Porous)

These two materials might not be the best representation of solar system bodies. However, in contrast to other materials, in both cases these material parameters have passed successful comparison tests with laboratory impact experiments (Benz and Asphaug 1995; Jutzi et al. 2009).

The initial conditions of the simulations presented here are summarized in Table 1. All the simulations were performed using 200,000 particles to model the parent body. The number of particles in the projectile was chosen to obtain the same mass per particle in the projectile as in the target.

Numerical Simulations of the Baptistina Family Formation

As we described when presenting the estimated properties from observations, the Baptistina family was first assumed to be a C-type one (Bottke et al. 2007). However, recent observations have indicated that it may be as well a S-type or even a mixture, although to our knowledge it would be the first family whose members do not all have the same taxonomic type. For this reason, we performed simulations of the Baptistina family formation using both a non-porous and a porous parent body. Note that Bottke et al. (2007) proposed a match of the real family with SPH-*N*-body simulations using non-porous parent bodies, and those simulations were performed on a 100 km-size object and rescaled to account for the 170 km-diameter of the Baptistina's parent body. Assuming that our codes and method are identical, our simulations can then also allow us to determine whether rescaling from a smaller target gives the same answer as if we start with the actual diameter of the parent body.

In this section, we present the results of our simulations. The implications regarding the real family will be discussed afterward.

Comparison to Previous Work: Non-Porous Parent Body

We start our investigations by using similar initial conditions suggested by Bottke et al. (2007).

By rescaling simulations performed using a non-porous parent body of diameter D = 100 km to the Baptistina case (D = 170 km), these authors found that a 60 km-diameter projectile impacting nearly vertically (impact angle of 15°) at 3 km s^{-1} could produce a reasonable match to the shape of the

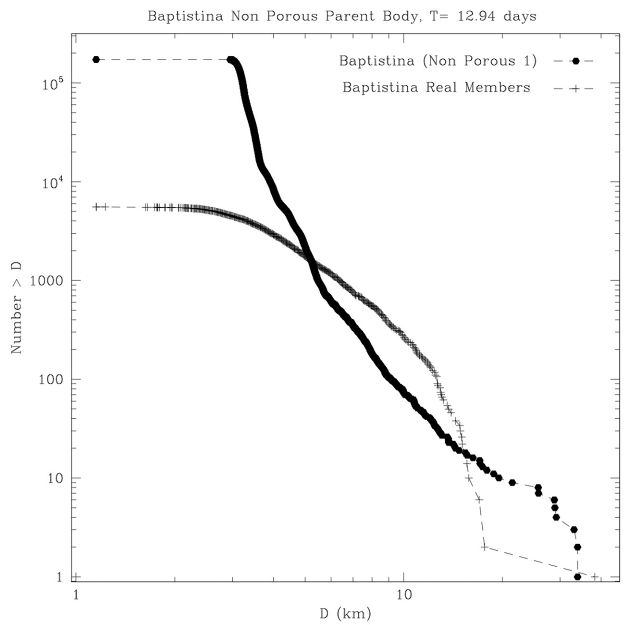

Fig. 1. Cumulative size distribution of fragments at the end of the gravitational phase from the simulation labeled Non-Porous 1 involving a 60 km-diameter projectile impacting at 0° (see Table 1). Note that the initial bulk density of both the target and the projectile is 2.7 g/cm^3. The size distribution estimated for the real family (Bottke et al. 2007) is indicated for comparison.

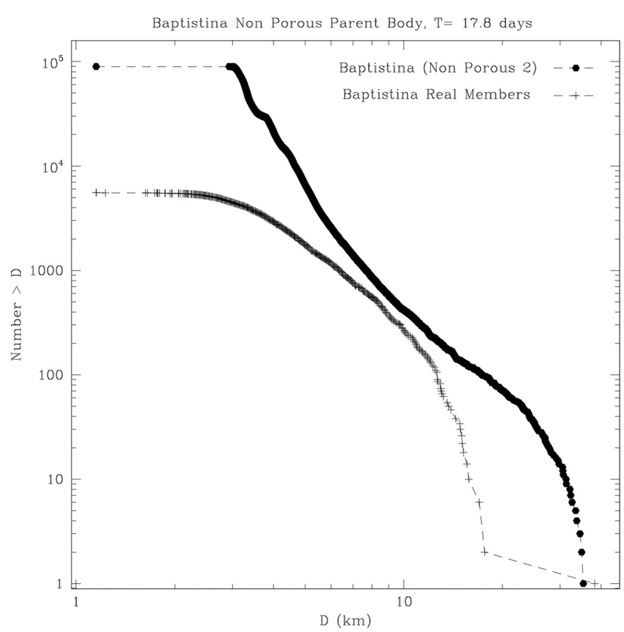

Fig. 2. Same as Fig. 1 for the Non Porous 2 simulation using a 88 km-diameter projectile impacting at 45° (see Table 1).

size distribution estimated for the real family. Their largest fragment remains smaller by a factor 1.6 than the estimated real one, but the authors noted that it comprises only 1% of the parent body's total mass, making this discrepancy almost meaningless. Figure 1 shows the cumulative size distribution of fragments at the end of the gravitational phase of our simulation using the same initial conditions as these authors (simulation Non-Porous 1), but this time starting directly with a 170 km-diameter parent body and using an impact angle of 0° instead of 15°. This plot should be compared with Fig. 2 of Bottke et al. (2007). We find that the size of the largest remnant as well as the global shape of the size distribution obtained in our simulation significantly differ from the model curve of Bottke et al. (2007). In particular, our simulation produces a largest remnant whose mass is closer to the estimated one for the real one, but it also produces a greater number of bodies of intermediate sizes. Simulating a head-on collision rather than a slightly off-center one (15° from vertical) may explain, at least partially, the reason for this difference. It may also be due to a different choice of parameters, such as the stepsize or the resolution. The impact regime is in this case very disruptive (the size of the largest remnant is only about 1% of the mass of the parent body), so the sensitivity to free parameters may be higher, and, in such a regime, the rescaling method may also break down. To verify this, a matrix of tests near the outcome of the simulation used by Bottke et al. (2007) before rescaling should be performed to check whether we can reproduce it in that way. This is beyond the scope of this current study, and is left for future investigations.

The most striking difference between the size distribution obtained by our simulation and the real one is the number of large fragments. While there is a large gap between the largest remnant and the smaller fragments in the observed family (causing a discontinuous shape of the distribution), this is not the case in the one produced by our simulation. In order to check whether such a discontinuity can be obtained by a non-head-on collision, we performed a simulation with an impact angle of 45° (Simulation Non-Porous 2). Note that the projectile in this case is larger (D = 88 km) than in the head-on impact, as an oblique impact requires more energy (by a factor of about three in this case; see Table 1) to achieve the same degree of disruption. Consequently, the average and mean ejection speeds of fragments also tend to be higher (Table 2). As Fig. 2 shows, the largest remnant has about the same size as the one produced by the head-on collision. Also the global

Table 2. Ejection speeds obtained in all our simulations. The label numbers of the models of parent bodies are the same as in Table 1. V_{ej}(Mlr) is the ejection speed of the largest fragment. $<V>$, V_{med} and V_{max} are the mean, median and maximum speeds (in m/s) of the fragments whose size is larger than the resolution of our simulations.

Model	V_{ej}(Mlr)	$<V>$	V_{med}	V_{max}
Non-porous 1	40	208	129	5953
Non-porous 2	224	287	153	5872
Porous 1	28	129	113	1462
Porous 2	37	140	123	1662
Porous 3	37	155	138	1718
Porous 4	65	176	158	1724
Porous 5	112	214	194	2042
Porous Ob	108	255	157	3583

shape is similar (continuous distribution) and the number of large fragments is even greater. However, a small range of sizes is better reproduced than from a head-on impact. As also recognized by Bottke et al. (2007), the parameter space being huge, we cannot rule out the possibility that other combinations of the impact conditions may lead to a discontinuous shape. However, here, being interested in the outcome produced by a porous parent body, we prefer to leave this problem open and concentrate on the differences produced by the two different models of parent body.

Non-Porous Versus Porous Parent Body

Before we show the results of a series of simulations using a porous parent body, we compare the outcome of simulations using a non-porous (Non-Porous 1) and a porous (Porous 5) parent body, respectively. In both cases, we use a projectile of D = 60 km. Since the composition of the projectile corresponds to the one of the target, this results in the same specific impact energy in both cases. Note, however, that due to the difference in density, the masses involved differ by a factor of two. Figure 3 shows the size distribution obtained from the porous model, to be compared with that obtained from the non-porous one in Fig. 1. We note that both the size of the largest remnant and the global shape of the distribution are significantly different. In particular, the simulation using a porous parent body provides a better qualitative match as it produces a discontinuous size distribution. The fact that the largest remnant is larger in the non-porous case might be surprising since laboratory impact experiments (e.g., Stewart and Ahrens 1999) indicate that porous bodies are stronger (i.e., more energy per mass unit is needed for disruption). However, preliminary studies (Michel et al. 2008) suggest that this is not necessarily true in the gravity regime where the bodies first get fully disrupted and the remnants form by gravitational reaccumulation.

For information, we indicate in Table 2 some statistical results on the fragment ejection speeds obtained in our simulations. The differences are difficult to interpret, as the impact energy regime is so disruptive that it can result in a wide variety of ejection velocity fields. Thus, we cannot easily determine some systematic trends as a function of impact energy or degree of disruption and we just note that the ejection speeds remain in the range of a few 100 m/s, as expected for this kind of event.

Simulations Using a Porous Parent Body

Assuming that the parent body was porous, as is expected for bodies of C taxonomic type, we performed a series of simulations using our model of fragmentation of porous material (simulations labeled Porous 1–5 and Porous Ob). By changing the specific impact energy, we searched for impact conditions that provided a best match to the estimated distribution of the real family. These simulations consisted of head-on impacts (impact angle of 0°), except one which consisted of using a 45° impact angle (simulation Porous Ob),

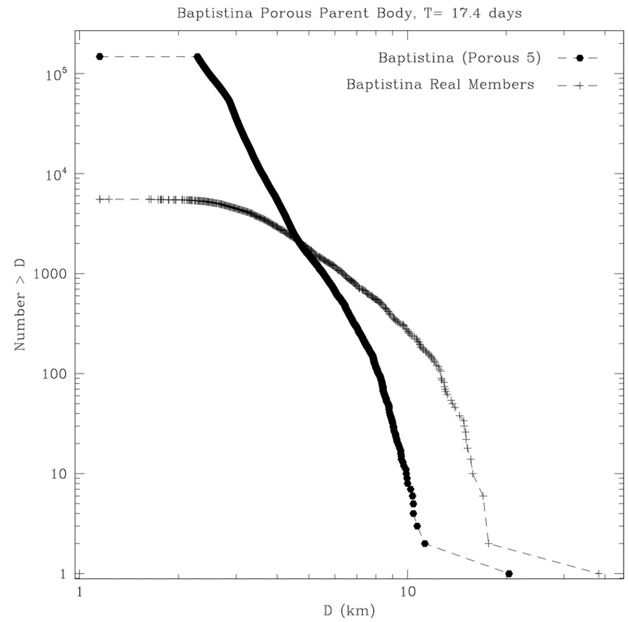

Fig. 3. Same as Fig. 1 from the simulation labeled Porous 5 using the same impact conditions as the simulation labeled Non-Porous 1 (see Table 1). Note, however, that the assumed bulk densities of both the target and the project are 1.3 g/cm^3 in the porous case, while instead they were set to 2.7 g/cm^3 in the non-porous one.

using different projectile sizes. Figure 4 shows the results of this exercise. As expected, the mass of the largest remnant decreases with increasing impact energy. Interestingly, the shape of the size distribution seems to change from continuous to discontinuous between the simulations Porous 3 and Porous 4. The mass of the largest remnant in the simulations with discontinuous size distributions (Porous 4 and 5) is smaller than the observed one. But if we accept the same level of discrepancy as the one used by Bottke et al. (2007), who had a factor 1.6 difference between their largest fragment and the real one, then we can consider in particular that our simulation labeled Porous 4 is a somewhat good match to the real family. This simulation involves a projectile of 27 km in radius (see Table 1).

The simulation using a 45° impact angle (Porous Ob) well reproduces the mass of the largest remnant but leads to a continuous size distribution.

DISCUSSION

As shown above, some of the size distributions (Porous 2 and Porous 6) obtained by our simulations have a mass of the largest remnant (see Table 1) that is comparable to the observed one, $M_{lr}/M_{pb} \approx 1.3 \times 10^{-2}$, where M_{lr} and M_{pb} are the mass of the largest remnant and the parent body, respectively. However, in these cases we find a rather continuous distribution instead of a discontinuous one as estimated for the real one. On the other hand, we do obtain some discontinuous size distributions in some models, but then we find a largest remnant which is too small compared to the estimated size of the real largest member

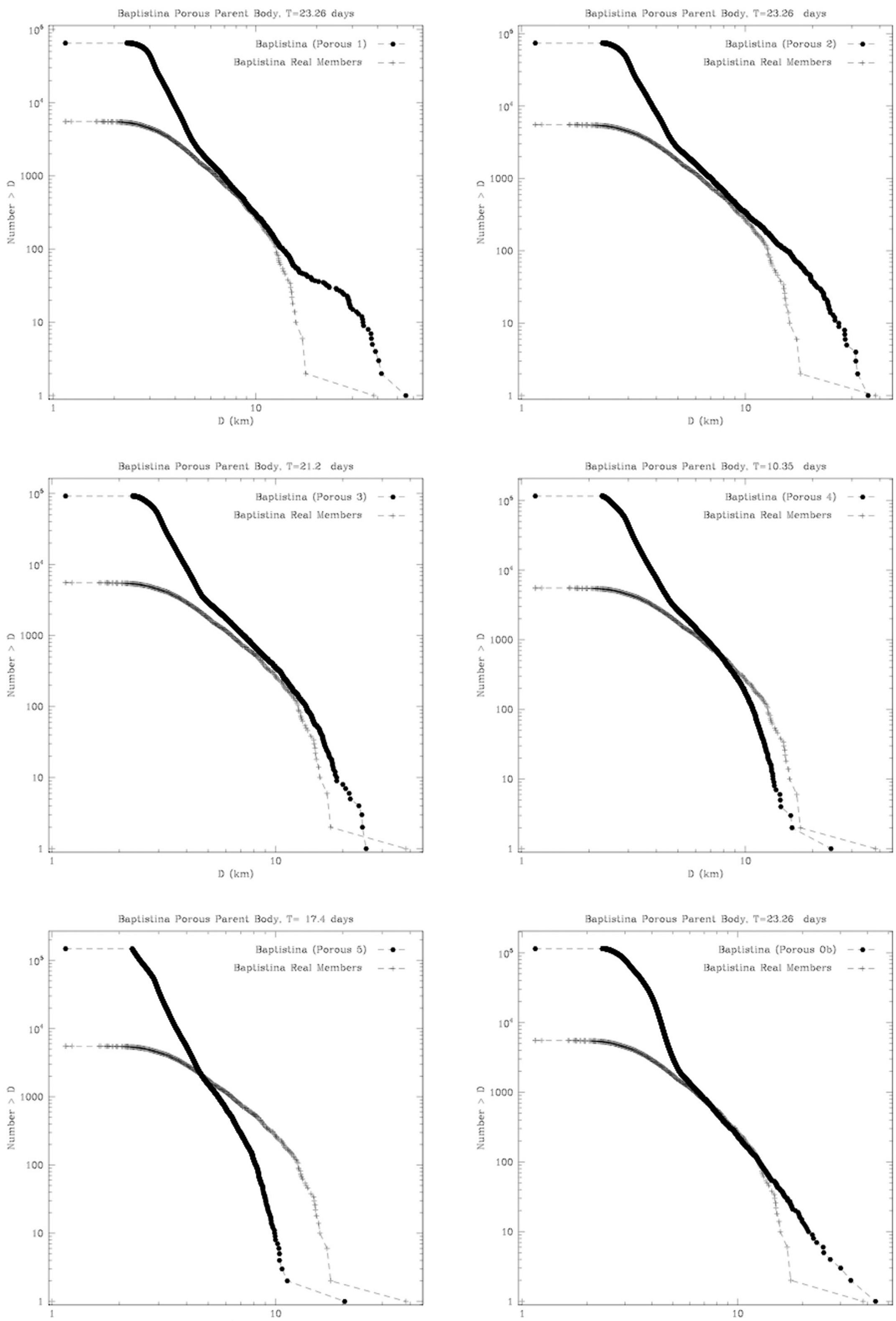

Fig. 4. Cumulative size distribution of fragments at the end of the gravitational phase from the simulations labeled Porous 1–5 involving various projectile sizes (the diameter increases with increasing label number; see Table I) impacting at 0°. The simulation labeled Porous Ob involves a projectile impacting at 45°.

of the family. As we said previously, we can probably consider that the discontinuous size distribution produced by our model labeled Porous 4 provides a reasonable match if we use the same degree of satisfaction as that used by Bottke et al. (2007), which had a mismatch between the diameters of their simulated largest remnant and the real one by a factor of 1.6 (see the section presenting the estimated properties of the family from observations).

Recent observations indicate that there may be more than one taxonomic type in the real family, and because families are generally very homogeneous, this indicates either that the parent body was a mixture, or more likely that there are interlopers. Therefore, it is likely that the real size distribution of the Baptistina family has a different shape, and thus it is too preliminary to consider that the differences we see in the ones we obtain with our simulations are of major concern.

Nevertheless, assuming that the Baptistina asteroid is not a C-type but rather closer to a S-type, and/or that its albedo is higher than the one currently used to estimate its diameter, then its estimated diameter would be reduced and the agreement with the simulation Porous 4, which produces a global shape similar to the real one, would be even better. Actually, Reddy et al. (2008) claim that 298 Baptistina has a 14% albedo, which would shrink it down to almost the size that we obtain in the simulation Porous 4. On the other hand we do not yet know the albedo of the objects in the full Baptistina family; if they have 14% albedo as well, nothing would change.

More observational data are required to conclude which of our simulations provide the best match to the real family, and we strongly urge our colleague observers to provide more data on this family. It is nevertheless already comforting that we can obtain different shapes and diameters of the largest remnant, which are the two things that may be revised by the observations.

CONCLUSION

We have presented the results of numerical simulations of the complete process of catastrophic disruption of a large asteroid aimed at representing the formation of the Baptistina family. Because there are still uncertainties about the actual taxonomic type of the family, we used both a non porous and a porous object to represent the family parent body. We then used two models of fragmentation included in our hydrocode, which are appropriate for each of these cases. The first one is the classical model of brittle failure used previously to reproduce asteroid families of bright taxonomic type (e.g., Michel et al. 2001, 2003); the second one is a model for porous material introduced recently in our hydrocode (Jutzi et al. 2008) and which passed a first validation at laboratory scale (Jutzi et al. 2009). The mutual attraction of generated fragments and their potential reaccumulations were then followed using the *N*-body code *pkdgrav*, as we did in our previous investigations of family formation (Michel et al. 2001, 2002, 2003, 2004a, 2004b).

Our results show that the break up of a porous body leads to different outcomes than the disruption of a non-porous one, in terms of both size and velocity distributions of the fragments. In particular, everything else being equal, a porous body appears weaker than a non-porous one. Because the bulk density of a porous body is smaller than that of a non-porous one, its mass is also smaller for the same diameter. In this regime where gravity dominates, the mass difference may at least partially explain why a porous body is weaker for the same impact energy and similar size as a non-porous one. We are currently performing a systematic study of the impact energy threshold for disruption of porous bodies which will allow us to determine whether this finding can be generalized.

From the disruption of a non-porous parent body, we find that our simulations tend to produce fragment size distributions that are generally more continuous than the one estimated from the observations (i.e., we generally find no gap between the largest and second-largest fragments). We then find that using a non-porous model starting directly with the appropriate size of the parent body does not lead to a good agreement with the properties of the real family estimated so far by the observations. In previous studies (Michel et al. 2002, 2004a) we usually found that highly catastrophic disruptions (such as the one at the origin of the Baptistina family) involving non-porous parent bodies favored the production of continuous fragment size distributions, and discontinuous ones were usually obtained for less energetic events. However, the parameter space is too large to cover it all, especially if we consider both the shape of the distribution and the size of the largest member to be robust, so we cannot rule out that some successful impact conditions involving a non-porous body may exist.

From the disruption of a porous parent body, some portions of the size distribution or the largest remnant mass can be well reproduced. In particular, break-ups of a porous body can produce a set of fragments whose size distribution is discontinuous even in such a highly catastrophic regime. We find that a head-on impact at 3 km s^{-1} of a projectile of 27 km in radius produces an outcome that can be considered as a reasonable match to the real family. Such a projectile's size is compatible with the scenario proposed by Bottke et al. (2007) about this family history.

Since our simulations provide a wide variety of outcomes depending on the impact conditions, when the real family properties become better constrained, it will then be easy to check on the results presented here whether some of them correspond to a better match and with which impact conditions and parent body. Such information is important, for instance to check or revise the estimated age of the family, which depends to some degree on the likelihood that the required impact conditions produced it.

The understanding of the impact response of a large body as a function of its internal properties is fundamental and asteroid families provide a good tool to improve it. In recent years, we have been able to validate our approach for non-porous parent bodies using well characterized bright family types, and we will repeat this exercise in future work with our model for porous materials using some well-characterized dark-type families. In this paper, we wanted to make a first application using the Baptistina family as an example, because of the recent finding by Bottke et al. (2007) about its role in the K/T impact, and our work can at least motivate observers to better characterize its properties.

Numerical simulations need well-determined properties both at laboratory scale and from observations at large scale. Then they can be validated and in turn provide important information on the conditions (impact energy, internal structure of the parent body) that can have produced the observed outcome. Obviously, the real material properties of the asteroids are not known yet, so that we are limited to using terrestrial analogs, but we can hope that future sample return missions, such as the Marco Polo mission, in assessment study at the European Space Agency, will provide some information about these properties, adding new constraints to our models.

Acknowledgments—M. J. and W. B. acknowledge support from the Swiss National Science Foundation. P. M. acknowledges the support of the French Programme National de Planétologie (PNP), the French Program Origine de Planètes et de la Vie (OPV), and the cooperation program CNRS-JSPS 2008–2009. D. C. R. acknowledges support from the grant NNX08AM39G (NASA).

Editorial Handling—Dr. Andy Rivkin

REFERENCES

Benz W. and Asphaug E. 1994. Impact simulations with fracture I. Method and tests. *Icarus* 107:98–116.

Benz W. and Asphaug E. 1995. Simulations of brittle solids using smooth particle hydrodynamics. *Computational Physics Communication* 87:253–265.

Bottke W. F., Vokrouhlický D., and Nesvorný D. 2007. An asteroid breakup 160 Myr ago as the probable source of the K/T impactor. *Nature* 449:48–53.

Britt D. T. and Consolmagno G. J. 2000. The porosity of dark meteorites and the structure of low albedo asteroids. *Icarus* 146: 213–219.

Bus S. J., Vilas F., and Barucci M. A. 2002. Visible wavelength spectroscopy of asteroids. In *Asteroid III*, edited by Bottke W. F., Cellino A., Paolicchi P., and Binzel R. P. Tucson, Arizona: The University of Arizona Press. pp. 169–182.

Carroll M. M. and Holt A. C. 1972. Suggested modification of the P–α model for porous materials. *Journal of Applied Physics* 43: 759–761.

Durda D. D., Bottke W. F., Enke B. L., Merline W. J., Asphaug E., Richardson D. C., and Leinhardt Z. M. 2004. The formation of asteroid satellites in large impacts: results from numerical simulations. *Icarus* 170:243–257.

Durda D. D., Bottke W. F., Nesvorný D., Enke B. L., Merline, W. J., Asphaug E., and Richardson D. C. 2007. Size frequency distributions of fragments from SPH/N-body simulations of asteroid impacts: Comparison with observed asteroid families. *Icarus* 186:498–516.

Grady D. E. and Kipp M. E. 1980. Continuum modeling of explosive fracture in oil shale. *International Journal of Rock Mechanics and Mining Science and Geomechanics Abstracts* 17:147–157.

Hermann W. 1969. Constitutive equation for the dynamic compaction of ductile porous materials. *Journal of Applied Physics* 40:2490–2499.

Housen K. R., Holsapple K. A., and Voss M. E. 1999. Compaction as the origin of the unusual craters on the asteroid Mathilde. *Nature* 402:155–157.

Ivezic Z. and 32 co-authors. 2001. Solar system objects observed in the Sloan Digital Sky Survey Commissioning Data. *The Astronomical Journal* 122:2749–2784.

Jutzi M., Benz W., and Michel P. 2008. Numerical simulations of impacts involving porous bodies I. Implementing sub-resolution porosity in a 3-D SPH hydrocode. *Icarus* 198:242–255.

Jutzi M., Michel P., Hiraoka K., Nakamura A. M., and Benz W. 2009. Numerical simulations of impacts involving porous bodies II. Comparison with laboratory experiments. *Icarus* 201:802–813.

Libersky L. D. and Petschek A. G. 1991. Smooth particle hydrodynamics with strength of materials. In *Proc. Next Free-Lagrange Methods, Lecture Notes in Physicics* 395, edited by Trease H. E., Fritts M. F., Crowley W. P., Berlin: Springer-Verlag. pp. 248–257.

Leinhardt Z. M. and Stewart S. T. 2009. Full numerical simulations of catastrophic small body collisions. *Icarus* 199:542–559.

Michel P., Benz W., Tanga P., and Richardson D. C. 2001. Collisions and gravitational reaccumulation: forming asteroid families and satellites. *Science* 294:1696–1700.

Michel P., Benz W., Tanga P., and Richardson D. C. 2002. Formation of asteroid families by catastrophic disruption: Simulations with fragmentation and gravitational reaccumulation. *Icarus* 160:10–23.

Michel P., Benz W., and Richardson D. C. 2003. Fragmented parent bodies as the origin of asteroid families. *Nature* 421:608–611.

Michel P., Benz W., and Richardson D. C. 2004a. Disruption of pre-shattered parent bodies. *Icarus* 168:420–432.

Michel P., Benz W., and Richardson D. C. 2004b. Catastrophic disruption of asteroids and family formation: A review of numerical simulations including both fragmentation and gravitational reaccumulation. *Planetary and Space Science* 52: 1109–1117.

Michel P., Jutzi M., Benz W., and Richardson D. C. 2008. Collisional family formation and scaling laws: Effects of porosity and explicit formation of spinning aggregates (abstract 55.09). *Bulletin of the American Astronomical Society* 40:499.

Mothé-Diniz T., Roig F., and Carvano J. M. 2005. Reanalysis of asteroid families structure through visible spectroscopy. *Icarus* 174:54–80.

Nesvorný D., Enke B. L., Bottke W. F., Durda D. D., Asphaug E., and Richardson D. C. Karin cluster formation by asteroid impact. *Icarus* 183:296–311.

Reddy V., Kelley M. S., Emery J. M., Gaffey J. M., Bottke W. F., Nesvorný D., Schaal M., Cramer A., and Takir D. 2008. Composition of 298 Baptistina: implications for K-T impactor link (abstract). Asteroids, Comets, Meteors 2008. CD-ROM.

Richardson D. C. 1994. Tree code simulations of planetary rings. *Monthly Notices of the Royal Astronomical Society* 269:493–511.

Richardson D. C., Quinn T., Stadel J., and Lake G. 2000. Direct large-scale N-body simulations of planetesimal dynamics. *Icarus* 143: 45–59.

Richardson D. C., Michel P., Walsh K. J., and Flynn K. W. 2009.

Numerical simulations of asteroids modeled as gravitational aggregates with cohesion. *Planetary and Space Science* 57:183–192.

Sirono S. 2004. Conditions for collisional growth of a grain aggregate. *Icarus* 167:431–452.

Stewart S. T. and Ahrens S. J. 1999. Porosity effects in impact processes on solar system materials (abstract #2020). 30th Lunar and Planetary Science Conference. CD-ROM.

Tillotson J. H. 1962. Metallic equations of state for hypervelocity impact. *General Atomic Report* GA-3216.

Wünnemann K., Collins G. S., and Melosh H. J. 2006. A strain-based porosity model for use in hydrocode simulations of impacts and implications for transient crater growth in porous targets. *Icarus* 180:514–527.

Yeomans D. K. Barriot J.-P., Dunham D. W., Farquhar R. W., Giorgini J. D., Helfrich C. E., Konopliv A. S., McAdams J. V., Miller J. K., Owen W. M., Jr., Scheeres D. J., Synnott S. P., and Williams B. G. 1997. Estimating the mass of asteroid 253 Mathilde from tracking data during the NEAR flyby. *Science* 278:2106–2109.